A PDZ scaffolding/CaM-mediated pathway in Cryptochrome signaling

A PDZ scaffolding/CaM-mediated pathway in Cryptochrome signaling

Bellanda Massimo[1#], Damulewicz Milena[2#], Zambelli Barbara[3], Costanzi Elisa[1], Gregoris Francesco[4], Mammi Stefano[1], Tosatto Silvio C.E.[4], Costa Rodolfo[5,6,7], Minervini Giovanni[4]*, Mazzotta Gabriella M.[5]*

[1]Department of Chemical Sciences, University of Padova, Padova, Italy; [2]Department of Cell Biology and Imaging, Jagiellonian University, Kraków, Poland; [3]Department of Pharmacy and Biotechnology, University of Bologna, Bologna, Italy; [4]Department of Biomedical Sciences, University of Padova, Padova, Italy; [5]Department of Biology, University of Padova, Padova, Italy. [6]Institute of Neuroscience, National Research Council of Italy (CNR), Padova, Italy; [7]Chronobiology Section, Faculty of Health and Medical Sciences, University of Surrey, Guildford, UK

* corresponding: giovanni.minervini@unipd.it; gabriella.mazzotta@unipd.it

# These authors contributed equally

Abstract

Cryptochromes are cardinal constituents of the circadian clock, which orchestrates daily physiological rhythms in living organisms. A growing body of evidence points to their participation in pathways that have not traditionally been associated with circadian clock regulation, implying that cryptochromes may be subject to modulation by multiple signaling mechanisms. In this study, we demonstrate that human CRY2 (hCRY2) forms a complex with the large, modular scaffolding protein known as Multi-PDZ Domain Protein 1 (MUPP1). This interaction is facilitated by the calcium-binding protein Calmodulin (CaM) in a calcium-dependent manner. Our findings suggest a novel cooperative mechanism for the regulation of mammalian cryptochromes, mediated by calcium ions (Ca^{2+}) and Calmodulin. We propose that this Ca^{2+}/CaM-mediated signaling pathway may be an evolutionarily conserved mechanism that has been maintained from Drosophila to mammals, most likely in relation to its potential role in the broader context of cryptochrome function and regulation. Further, the understanding of cryptochrome interactions with other proteins and signaling pathways could lead to a better definition of its role within the intricate network of molecular interactions that govern circadian rhythms.

Keywords: hCRY2, MUPP1, Calmodulin, circadian rhythms, cryptochrome signaling.

Introduction

Cryptochromes are flavin-containing blue light photoreceptors related to photolyases, DNA-repair enzymes that use blue light to repair UV induced DNA damage. Cryptochromes have been described in various animal lineages, including insects, fish, amphibians and mammals[1]. They have lost the DNA repair activity and have been recruited by the circadian machinery, either as components of the mechanism generating the circadian oscillation and controlling the daily behavioral/physiological rhythms, or as photoreceptors mediating the entrainment of the circadian clock to light[2].

Cryptochromes have acquired an intrinsically unstructured C-terminal extension that participates, to varying degrees in their circadian functions. In Drosophila, Cryptochrome (CRY) has a well-established role in mediating the response to light and regulating light-dependent interactions with target proteins[3–7], while in vertebrate-like cryptochromes its function is less defined, although several pieces of evidence support the hypothesis that it might be implicated in protein stability, ultimately affecting circadian rhythmicity[8,9]. Drosophila CRY, exhibits a wide panoply of functions (reviewed in[10]): it acts as the primary blue light photopigment that mediates circadian responses to light[11–18] and evidence is accumulating on its role in light-dependent magneto-sensitive responses[19–23]. Moreover, CRY appears to be an integral component of the molecular clock in peripheral tissues, including the compound eyes[24–26], where we have previously shown it to play a role independent on light activation[27]. Vertebrate cryptochromes have apparently lost the ability to sense light and have been recruited as light-independent negative autoregulators of the circadian clock[28–33]. There is evidence to suggest the involvement of mammalian CRYs in several additional signaling pathway, to include acting as second messengers between the core clock and other cellular processes, such as maintenance of cellular and genomic integrity and metabolism[34–38]. Nevertheless, the nature of the transduction signaling involving CRYs remains largely unknown. We have previously shown that dCRY acts through Inactivation No Afterpotential D (INAD) in a light-dependent manner on the Signalplex, a multiprotein complex that includes visual-signaling molecules[39]. Furthermore, we have identified and characterized a Calmodulin (CaM) binding motif in the dCRY C-terminus[40]. Similarly, we also defined the CaM binding site of the scaffold protein INAD and demonstrated that CaM bridges dCRY and INAD to form a ternary complex in vivo, suggesting a process in which a rapid dCRY light response stimulates an interaction with INAD, that can be consolidated by a novel mechanism regulated by CaM[40]. The intracellular signaling machinery is often organized around scaffolding proteins localized at the plasma membrane, and multiple PDZ proteins bind to the various constituents of the transduction pathway, bringing them into close proximity and precisely defined stoichiometry, ultimately ensuring a rapid and specific signal transduction[41]. Based on the hypothesis that evolution has conserved in mammals a mechanism similar to the one known for Drosophila, we searched for common components between mammals and insects, to shed light on the mechanisms involved in mammalian clock entrainment. Thus, firstly we performed bioinformatics analyses to identify putative scaffolding proteins able to interact with mammalian CRYs. We then performed *in vitro* validations to confirm the interaction between the molecular components suggested to be binding partners.

Results

MUPP1 identification and its interaction with hCRY2

In a previous study, we demonstrated that an INAD fragment, including the PDZ2, its upstream region, and PDZ3 domains (residues 207- 448) is crucial for its association with dCRY[39]. To identify an INAD functionally related protein in mammals, we performed a pBlast search against the UniProt database. Initially, the PDZ3 of INAD was employed as the query in our search, focusing on mammalian proteins which led to the identification of multiple MUPP1 orthologue proteins. Subsequently, this search was further refined by employing the same query against the SwissProt database resulting in the isolation of human proteins. Among the outcomes, the highest-scoring match (Max score: 106, e-value 3e-26, Percent Identity: 31.69%) corresponded to the human MUPP1

(UniProt ID: O75970). MUPP1 is a 13 PDZ tandem domains containing protein differentially expressed in several mouse tissues, such as brain, skeletal muscle, heart, liver kidney and lung[42]. It is particularly abundant in the brain, where it localizes at the junctions of epithelial and endothelial cells and at the neuronal synapses[43–48]. Research in humans and animal models has uncovered several essential neuronal functions for this large modular scaffolding protein, which has been proposed to participate in the N-methyl-D-aspartic acid receptor (NMDAR) signaling and to play a role in the regulation of synaptic plasticity[49]. We then wondered which PDZ domain of hMUPP1 shows the highest sequence similarity with the pair formed by INAD PDZ2 and PDZ3. The best matches were obtained by aligning INAD-PDZ2 against hMUPP1-PDZ8 (40% similarity) and INAD-PDZ3 against hMUPP1-PDZ9 (30% similarity). High sequence similarity (70%) was also found between the INAD PDZ2 upstream region (residues 207-248) and the corresponding hMUPP1-PDZ8 upstream region (Figure 1A). Furthermore, we found that both INAD and MUPP1 share a conserved sequence pattern ([DE]-[DE]-EDEFGY[TS][MW]--I--RY--[ML]---L) localized in a predicted disordered region (Figure 1A), suggesting that MUPP1 may play a role similar to that of INAD. The physical interaction between hCRY2 and MUPP1 was analyzed by a yeast two hybrid assay, in which a full-length hCRY2, directly fused to LexA (bait), was challenged with a 257 aa fragment of hMUPP1 (aa 1307-1564_ UNIPROT O75970), comprising PDZ domains 8 and 9 and the upstream region, homologue to PDZ 2-3 of INAD. hCRY2 was observed to interact with hMUPP1 independently from light (Figure 1B).

MUPP1 and CaM: details of an interaction

Through bioinformatics analysis, we predicted the existence of a putative CaM binding site within the conserved motif. Specifically, this site is identified as non-canonical and exhibits characteristics of the "1-12 motif," characterized by the presence of two conserved bulky hydrophobic residues separated by a series of variable amino acids (https://cam.umassmed.edu). The physical interaction between MUPP1 and CaM was analyzed by using several approaches. In a yeast two-hybrid assay, the full-length protein (CaM_{1-149}) and separate domains (CaM_{1-80} and CaM_{75-149}) were challenged with $hMUPP1_{1307-1564}$. The results show an interaction between the two proteins, which is preferentially mediated by the C-terminal lobe of CaM (Figure 2A). To further elucidate the novel interaction between MUPP1 and CaM, we synthesized a short peptide encompassing residue 1331-1343 of MUPP1 and containing the predicted binding site ($MUPP1_{1331-1343}$). $MUPP1_{1331-1343}$ addition to CaM in the presence of 5 mM Ca(II) or 5 mM EGTA was followed using isothermal titration calorimetry (ITC). A binding event of the peptide to the protein was revealed to be Ca(II) dependent, as exothermic peaks followed each addition in the presence of the Ca(II) ion, while no heat effect was visible in presence of EGTA (Figure 2B top panel). Fits of the integrated heat produced a titration curve with two inflection points, which could not give a good fit with a single binding event model. Thus, a two sets of independent sites model was used (Figure 2B, bottom panel), which produced a good fit ($\chi^2 = 456.2$), entailing two binding sites per CaM monomer with affinities that differ by two orders of magnitude: $K_{A1} = 2.4 \pm 0.1 \times 10^6$ ($K_{B1} = 0.43 \pm 0.02$ μM) and $K_{A2} = 1.5 \pm 0.1 \times 10^4$ ($K_{B2} = 67 \pm 4$ μM). Both binding events are enthalpically driven ($\Delta H_1 = -9.41 \pm 0.01$ kcal mol^{-1} and $\Delta H_2 = -7.53 \pm 0.01$ kcal mol^{-1}) and presented negative entropy ($\Delta S_1 = -2.41$ kcal mol^{-1} K^{-1} and $\Delta S_2 = -6.09$ kcal mol^{-1} K^{-1}). We used heteronuclear two-dimensional nuclear magnetic resonance (2D NMR) to define the portion of CaM involved in the binding with MUPP1. Specifically, we titrated ^{15}N-labeled CaM with up to a 2.5 fold molar excess of unlabeled $MUPP1_{1331-1343}$ and we acquired several ^{15}N-HSQC at different protein-peptide ratios. The ^{15}N-HSQC spectrum represents a fingerprint of the

protein where, as a first approximation, every peak corresponds to a residue. The peaks in the HSQC map are very sensitive to the chemical environment of the corresponding amino acid and therefore this experiment represents a useful tool to study the interaction of a protein with other molecules, at an atomic level: protein residues involved in the interaction will undergo significant changes upon binding of the molecule. To use this tool, the assignment of the ^{15}N-HSQC spectrum should be obtained first. The resonance assignment of CaM ^{15}N-HSQC had been previously achieved by a set of triple resonance NMR experiments acquired on the ^{13}C,^{15}N-CaM[40]. The ^{15}N-HSQC spectra of CaM in the presence of increasing amounts of MUPP1$_{1331-1343}$ are reported in Figure 2C, which shows that a large number of peaks are affected upon addition of the peptide. In the first part of the titration, a number of peaks become weaker, and ~~they~~ completely disappear upon addition of one equivalent of peptide with respect to calmodulin. Further, we also compared the spectrum in presence of 0.6 equivalents of MUPP1$_{1331-1343}$ (Figure 2C, blue peaks,) against the free CaM (red peaks) and concluded that the free protein is significantly decreased upon addition the MUPP1 peptide. Notably, all the signals showing this behavior correspond to the C-terminal lobe of CaM. At the same time, new signals appear in the spectrum, and they increase in intensity until a 1:1 molar ratio is reached, after which they remain substantially unchanged (Figure 2C, yellow peaks), whereas the same peaks significantly shift upon addition of 2 equivalents of the peptide (cyan peaks). On the contrary, peaks from the C-terminal domain of CaM are sharp at 1 equivalent of MUPP1$_{1331-1343}$ and they undergo only minor changes upon further addition of the peptide. When 2 equivalents of peptide are added, peaks become sharper while no further changes were observed over 2.5 equivalents of MUPP1$_{1331-1343}$ (Figure S1 and S2). This observation clearly indicates an interaction between CaM and MUPP1$_{1331-1343}$ characterized by a slow exchange regime in the NMR timescale and associated therefore to a strong binding between the two macromolecules. In these conditions, it is not possible to derive the assignment of the peptide-bound calmodulin from that available for the free form. Anyway, the residues affected by this first binding event can be identified by monitoring the changes in intensity for the peaks of free calmodulin during the first part of the titration. By comparing the ^{15}N-HSQC spectra of CaM in the absence and in the presence of 0.6 equivalents of MUPP1$_{1331-1343}$, it is evident that all the peaks of free CaM showing a large decrease of their intensity correspond to residues of the C-terminal lobe of the protein (Figures 2C and S3). On the contrary, peaks belonging to the N-terminal domain show only small changes in their position or intensity at this point of the titration (Figures 2C and S3). This observation strongly suggests a preferential interaction of MUPP1 with the C-terminal domain of calmodulin as indicated also by yeast two-hybrid experiments (Figure 2A). By further increasing the amount of MUPP1$_{1331-1343}$, also many signals of the N-terminal domain of CaM were significantly perturbed. In particular, they started shifting and becoming broad in the presence of 1 equivalent of peptide and then progressively got narrower and moved to a different position of the spectrum in the second part of the titration, until 2 equivalents of peptide were added (Figure 2C). No significant changes were observed by further increasing the amount of MUPP1$_{1331-1343}$ (Figure 2C). This behavior is consistent with a second binding site for MUPP1$_{1331-1343}$ localized on the N-terminal domain of calmodulin. This second binding event is characterized by an intermediate exchange regime in the NMR timescale and therefore by a lower affinity compared with the one described above for the C-terminal lobe. The results of these NMR experiments are fully in agreement with those independently obtained by ITC and previously described. An in-vitro CaM pulldown assay was performed in the presence or absence of Ca^{2+}, to investigate whether binding of hMUPP1 and CaM is Ca^{2+}-dependent. Protein extracts from HEK-293T cells overexpressing a MYC-tagged form of hMUPP1 were incubated with CaM Sepharose beads and the bound proteins were

analyzed by western-blot. The result shows that hMUPP1 binds CaM in a Ca^{2+}-dependent manner (Figure 2D).

CaM forms a ternary complex with hCRY2 and MUPP1

Given that the interaction between hMUPP1 and CaM seems to be mediated by the C-terminal lobe of CaM, we wondered whether it could bridge hMUPP1 to hCRY2, as we have previously observed with the Drosophila counterparts[40]. In a yeast two-hybrid assay, in which we have challenged the hCRY2 with CaM, either as full-length protein ($CaM_{1–149}$) or as separate domains ($CaM_{1–80}$ and $CaM_{75–149}$), we observed a preferential interaction between hCRY2 and the N-terminal lobe of CaM, which strengthens our hypothesis (Figure 3A). In other words, this result suggests that calmodulin may undergo a conformational change in which one of the two partners is bound first, and this interaction then leads to the formation of a ternary complex between hCRY-CaM and MUPP1. We then performed a CoIP assay, in which protein extracts from Drosophila S2R+ cells overexpressing HA-CRY2, $MUPP1_{1307-1564}$-HIS and MYC-hCAM full-length (input) were subjected to immunoprecipitation with anti-HA high affinity matrix and probed in Western blot with anti-HA, anti-HIS and anti-MYC. A signal in the "BOUND" sample for either anti-HIS or anti-MYC revealed that both $hMUPP1_{1307-1564}$ and hCaM were bound to hCRY2; however, bands in the "UNBOUND" samples for both constructs indicate that not the total amount of the proteins was involved in the binding. Overall, our results reveal that a ternary complex, hCRY2-CaM-$MUPP1_{1307-1564}$ is formed (Figure 3B).

Discussion

In this study, we have identified the mammalian protein MUPP1 as having a functional connection to INAD, a protein involved in the CRY mediated light signaling to the circadian clock in Drosophila and discovered that MUPP1 has a high sequence similarity with INAD in PDZ domains 2 and 3 and the upstream region of PDZ2. MUPP1 (multi-PDZ domain protein 1), also known as DLG3 (discs large homolog 3), is a protein that plays a crucial role in the organization and function of protein complexes at the plasma membrane[42,43]. It contains multiple PDZ domains, which are protein-protein interaction domains that bind to specific short amino acid sequences, and it can interact with a variety of proteins including ion channels, receptors, and cytoskeletal proteins[43,44]. PDZ domain proteins are involved in a wide range of cellular processes, including signal transduction, cell adhesion, and protein trafficking. They are found in all eukaryotes and are particularly abundant in the nervous system, where they play important roles in the regulation of synaptic signaling and plasticity. PDZ domains and calmodulin are two distinct protein domains that can interact with each other in various cellular processes. Calmodulin has been shown to interact with several PDZ domain-containing proteins, including the MAGUK family of proteins (membrane-associated guanylate kinase) such as PSD-95 and SAP97[44,46]. These interactions can regulate the localization and activity of these proteins at the plasma membrane, and thereby regulate various signaling pathways. For example, the interaction between Calmodulin and PSD-95[47] can regulate the clustering of NMDA receptors at synapses, which is important for synaptic plasticity and learning and memory. Overall, the interaction between PDZ domains and calmodulin is an important mechanism for regulating protein-protein interactions and signaling pathways in various cellular processes. Identifying MUPP1 as functionally related to INAD offers insights into the conservation of circadian clock mechanisms across species. We explored the physical interaction between MUPP1 and hCRY2, finding that they interact in a

light-independent manner. We also demonstrated a Ca^{2+} dependent MUPP1 interaction with CaM using biochemical and biophysical techniques. Isothermal titration calorimetry showed that two independent binding sites on CaM are involved, with affinities differing by two orders of magnitude (K_D = 0.43 – 67 μM). Differently, INAD was found to bind CaM with a 1:1 stoichiometry and lower affinity (K_D = 164 μM). This result was fully confirmed by heteronuclear 2D NMR, which also demonstrated that the association with MUPP1 is primarily mediated by CaM C-terminal lobe. This domain binds MUPP1 with high affinity and only when it is largely saturated, the interaction occurs also with the N-terminal lobe of CaM. This observation suggests that when MUPP1 is bound to CaM through its C-terminal domain, the N-terminal lobe remains available for an interaction with a different protein partner. We experimentally showed that CaM forms a ternary complex with hCRY2 and MUPP1 in vitro, suggesting that CaM may serve as a bridge between the proteins (Figure 4), analogously to what we have observed for the Drosophila orthologues[40]. The interactions between hCRY2 and MUPP1 and the ternary complex formation with CaM imply that MUPP1 may contribute to circadian clock regulation by modulating hCRY2 activity. Identifying MUPP1 as a factor potentially involved in the regulation of the mammalian circadian clock implies that this mechanism may be conserved, despite protein differences, and that the interaction between hCRY2, CaM and MUPP1 is part of the intricate network of intracellular signals that regulate and are regulated by the clock. Mammalian circadian clocks are primarily synchronized by light, detected by retinal photoreceptors and transmitted to the brain's master clock. However, several pieces of evidence indicate that they can be modulated by multiple other signaling pathways. The key role of Ca^{2+} signaling in the modulation of circadian clocks is established, with the calcium ion (Ca^{2+}) being known to maintain molecular rhythmicity by regulating the expression of clock genes as Per1, Per2 and Bmal1[50–52] and the stability and cellular localization of clock proteins such as PER2[53]. This study offers valuable insight into the interactions between proteins involved in circadian signaling and proposes a Ca^{2+}/CaM-mediated mechanism regulating mammalian CRYs[2].

Conclusions

This study has identified a functional connection between the mammalian protein MUPP1 and INAD, a protein involved in clock signaling in Drosophila. The study shows that MUPP1 interacts with hCRY2 and CaM in a light-independent manner, suggesting that MUPP1 may contribute to circadian clock activity by modulating hCRY2. Although future research is needed to examine their functional outcomes, the discovery of these interactions identifies a potential cooperative mechanism explaining how intracellular signals transmit time information to the host and, in turn, how they can be affected by the host's physiology.

Materials and Methods

Bioinformatic analysis

MUPP1 was obtained through p-BLAST search from the non-redundant (NR) database. Conservation analysis was performed using Jalview[54] with T-Coffee[55] and a BLOSUM62 matrix. Intrinsic disordered regions of the hMUPP1 and INAD were predicted with Cspritz[56]. ELM[57] was used to identify PDZ interaction motifs in mammalian CRY2 CTTs. A sequence logo was built with Weblogo[58]. Protein sequences used for these analyses were retrieved from Uniprot[59] and presented as following. Uniprot ID – INAD: *D. melanogaster* (Q24008), *D. sechellia* (B4I8C5), *D. simulans*

(B4QI19), *D. yakuba* (B4P8L2), *D. erecta* (B3NNX5), *D. persimilis* (B4H514), *D. mojavensis* (B4KSL1), *D. virilis* (B4LMW1), *D. willistoni* (B4MJM0), *D. grimshawi* (B4J763), *D. pseudoobscura* (Q28X50), *D. ananassae* (B3MEK4). MUPP1: *Homo sapiens* (O75970), *Mus musculus* (Q8VBX6), *Rattus norvegicus* (055164), *Pan troglodytes* (Chimpanzee) (H2R430), *Bos taurus* (Bovine) (F1MMT3), *Macaca mulatta* (Rhesus macaque) (F6T1W3), *Equus caballus* (Horse) (F6S559), *Ailuropoda melanoleuca* (Giant panda) (G1L4U6), *Canis familiaris* (Dog) (F1PGB9), *Callithrix jacchus* (White-tufted-ear marmoset) (F7FYD6), *Oryctolagus cuniculus* (Rabbit) (G1SLR4), *Mustela putorius furo* (ferret) (M3XYK5), *Sus scrofa* (Pig) (F1SMP5), *Myotis lucifugus* (Little brown bat) (G1P3E1), *Felis catus* (Cat) (M3WF73), *Otolemur garnettii* (Small-eared galago) (H0WTI1), *Pongo abelii* (Sumatran orangutan) (H2PS57). CRY2: *Mus musculus* (Q9R194), *Homo Sapiens* (Q49AN0), *Rattus norvegicus* (Q92318), *Pan troglodytes* (Chimpanzee) (H2Q3H0), *Bos taurus* (Bovine) (F1N0J9), *Macaca mulatta* (Rhesus macaque) (F7HH05), *Equus caballus* (Horse) (F6Y7Z4), *Ailuropoda melanoleuca* (Giant panda) (G1L1K6), *Canis familiaris* (Dog) (F1PNC9), *Callithrix jacchus* (White-tufted-ear marmoset) (F6RC52), *Oryctolagus cuniculus* (Rabbit) (G1THJ9), *Mustela putorius furo* (ferret) (M3Y337), *Sus scrofa* (Pig) (F1SHJ9), *Myotis lucifugus* (Little brown bat) (G1PQN8), *Felis catus* (Cat) (M3VZW3), *Otolemur garnettii* (Small-eared galago) (H0X769), *Pongo abelii* (Sumatran orangutan) (H2NDL2). The presence of putative calmodulin binding sites was investigated with the Calmodulin target Databases[60].

Yeast Two-Hybrid Assays

The experiments were performed in the EGY48 yeast strain (MATα, *ura*3, *trp*1, *his*3, 3LexA-operator-LEU). Baits were prepared by cloning the sequence of interest fused to the LexA moiety in the bait vector (pEG202), while preys contained the desired proteins fused to the "acid-blob" portion of the prey vector (pJG4-5)[61].

The full-length hCry2 bait was described in [27]. The CaM constructs (bait or prey) were described in[40]. The hMUPP1 fragment comprising aa 1307-1620 was amplified from pCMV6_entry_MPDZ_Myc_DDK tagged (plasmid # RC219952 from Origene_ Rockville, MD, USA) with the primers pJG_hMUPP_F (5'-GTGCCAGATTATGCCTCTCCCGAATTCATGGAAATGGGTAGTGATCACACACAG-3') and pJG_hMUPP_R (5'-CGAAGAAGTCCAAAGCTTCTCGAGCATATGTCAGCAGGTTGCAGGATCAGAAGC-3').

The cloning was performed by using the In-Fusion® HD Cloning Kit (Clontech, Mountain View, CA, USA) and the construct fully sequenced to assess the in-frame insertion of the cDNA and to control for unwanted mutations. Quantification of β-galactosidase activity was performed in liquid culture by the Miller assay, as in [63]. One Miller unit corresponds to a standardized amount of β-Gal activity. A student's t-test was used to perform single group comparisons.

Co-IP and western blot

The full length hCry2 and hCaM coding sequences and the hMUPP1 fragment comprising aa 1307-1620 were cloned into S2 expression vector pAC5.1/V5-His (Thermo Fisher Scientific, Waltham, MA, USA). hCry2 coding sequence was amplified from pSO2002 plasmid[2(p2)] 63 by pAc_HA_hCRY2F (5'-CAGTGTGGTGGAATTCATGTACCCATACGATGTTCCAGATTACGCTGCGGCAACTGTGG CAACGGC-3'), that adds a HA tag at the 5' of the coding sequence, and pAc_HA_hCRY2R (5'-GACTCGAGCGGCCGCTCAGGCATCCTTGCTCGGCAG-3'). hCaM coding sequence was

amplified from Universal Human Reference RNA (Thermo Fisher Scientific, Waltham, MA, USA), by pAct-hCaM-MYC-F (5' CAGTGTGGTGGAATTCATGGAACAAAAACTCATCTCAGAAGAGGATCTGGCTGATCAG CTGACCGAAGAAC-3') that adds a MYC tag at the 5' of the coding sequence and pAct-hCaM-R (5'-TAGACTCGAGCGGCCGCTCATTTTGCAGTCATCATCTGTAC-3'). The hMUPP1(1307-1620) was amplified from plasmid # RC219952 with the primers pAc_hMUPP1F (5'-GTGCCAGATTATGCCTCTCCCGAATTCATGGAAATGGGTAGTGATCACACACAG-3') and pAc_hMUPP1R (5'- GACTCGAGCGGCCGCAAGCAGGTTGCAGGATCAGAAG -3'), in frame with the HIS-tag present in the vector downstream the cloning site. The cloning was performed by using the In-Fusion® HD Cloning Kit (Clontech, Mountain View, CA, USA) and the constructs fully sequenced to assess the in-frame insertion of the cDNA and to control for unwanted mutations. Drosophila S2R+ cells, maintained at 25 °C in Schneider's Drosophila medium (Thermo Fisher Scientific, Waltham, MA, USA) added with 10% FBS (Gibco_Thermo Fisher Scientific, Waltham, MA, USA) were co-transfected by using using the Effectene Transfection Reagent (Qiagen, Gaithersburg, MD, USA), following manufacturer instruction. Cell extracts were subjected to coimmunoprecipitation (CoIP) by using an anti-high affinity (anti-HA) Affinity Matrix (Roche, Basel, CH), following manufacturer instructions. SDS PAGE was performed as previously described in [39] and immunocomplexes were analyzed using a mouse anti-HIS (1:2000; Qiagen, Gaithersburg, MD, USA), a mouse anti-HA (1:2000; Sigma Aldrich, St. Louis, MO, USA) and a mouse anti-MYC (1:2000; Sigma Aldrich, St. Louis, MO, USA) as primary antibodies and an anti-mouse IgG HRP (1:5.000; Sigma Aldrich, St. Louis, MO, USA) as secondary antibody.

CaM Pulldown Assay

Human embryonic-kidney 293T (HEK-293T) cells, maintained at 37°C in Dulbecco's Modified Eagle's Medium (DMEM) (Thermo Fisher Scientific, Waltham, MA, USA) added with 10% FBS (Gibco_Thermo Fisher Scientific, Waltham, MA, USA), were transfected with 2 mg of pCMV6_entry_MPDZ_Myc_DDK (hMUPP1) using Lipofectamine-2000 (Thermo Fisher Scientific, Waltham, MA, USA) following manufacturer instruction. Briefly, DNA was pre-complexed with Lipofectamine-2000 at a ratio of 1:3, in serum-free medium for 15 min at room temperature. The complex medium was added to the cells and incubated for 4 h at 37 °C before being replaced with DMEM plus 10% FBS. Cells were collected after 24 hours. Protein extraction and CaM pulldown assay were performed as described in [40]. CaM bound proteins were detached from the beads by the addition of loading buffer (LDS_ Thermo Fisher Scientific, Waltham, MA, USA) and heating at 75 °C for 10 min and analyzed by SDS-PAGE on 3%–8% NuPAGE Tris-Acetate Gels (Thermo Fisher Scientific, Waltham, MA, USA). Western Blot was performed with monoclonal anti-MYC antibody (1:2.000, Clontech, Mountain View, CA, USA) and anti-mouse IgG HRP secondary antibody (1:5.000; Sigma Aldrich, St. Louis, MO, USA).

Calmodulin expression and purification

Unlabeled and ^{15}N-isotopically labeled samples of calmodulin from *Xenopus laevis* (with identical amino acid sequence of human CaM) were recombinantly produced in *E. coli* BL21(DE3) cells grown in LB (unlabeled protein) or in M9 minimal medium containing 4.4 g/L glucose monohydrate and 1 g/L $^{15}NH_4Cl$ (^{15}N-labeled protein) with 50 µg/mL kanamycin for selection. Cells were grown at 37 °C and induced overnight at 20 °C. Bacteria were suspended in 50 mM Tris-HCl pH 7.5, lysed and the soluble fraction was mixed with 5 mLof Phenyl FF resin (GE Healthcare, Chicago, IL, USA) in

ice for 1 h and 15 min to remove highly hydrophobic proteins. The resin was centrifuged for 15 min, at 5000g, 4 °C, the supernatant was filtered and CaCl2 was added at a final concentration of 5 mM before loading onto into a series of two Phenyl Sepharose HP, 5 mL columns (GE Healthcare, Chicago, IL, USA) equilibrated with 50 mM Tris-HCl buffer, 1 mM CaCl2, pH 6.5. Calmodulin was eluted with 50 mM Tris-HCl buffer, 1 mM EGTA, pH 6.5 and further purified by means of a Superdex 75 prep-grade 16/60 (GE Healthcare, Chicago, IL, USA) SEC column equilibrated with 50 mM Tris-HCl, 150 mM NaCl, pH 7.5. Pooled samples were concentrated at 20–30 mg/mL, and flash-frozen in liquid nitrogen for further analysis.

Peptide synthesis

The $MUPP1_{1331-1343}$ peptide (purity > 99%) was purchased from Thermo Fisher Scientific (Waltham, MA, USA). The peptide was acetylated at the N-terminus and amidated at the C-terminus, to mimic the protein environment and remove extra charges.

Nuclear Magnetic Resonance (NMR) experiments

All NMR experiments were performed with a Bruker DMX 600 MHz spectrometer with a room temperature probe, at 303 K. ^{15}N-HSQC experiments were collected with 8 scans, 2048 complex data points and a spectral width of 14 ppm in the ^{1}H dimension, and 200 increments and a spectral width of 25 ppm in the ^{15}N dimension. Samples of 340-380 µM uniformly ^{15}N-labeled CaM were titrated with peptide stock solutions (3.2 mM $MUPP1_{1331-1343}$). The protein and the peptide were dissolved in the same buffer consisting of 50 mM Tris-Cl, 100 mM NaCl, 5 mM $CaCl_2$ at pH 6.5. The pH of the solutions was checked and adjusted after dissolving calmodulin and the peptides, to avoid pH changes during the titration. Deuterated water (10 % v/v) was added to the NMR tube. Resonance assignment of the ^{15}N-HSQC for the Ca^{2+} loaded apo-CaM spectrum in these experimental conditions was achieved as previously described[40]. Data were processed with TOPSPIN 3.1 (Bruker BioSpin GmbH, Rheinstetten, DE) and analyzed using CARA 1.9 (Keller) and NMRFAM-Sparky[64].

Isothermal titration calorimetry

Isothermal titration calorimetry (ITC) experiments were performed using a high-sensitivity VP ITC microcalorimeter (MicroCal LLC, Northampton, MA, USA). The reference cell was filled with deionized water. Protein and peptide solutions were prepared by diluting concentrated stock solutions in the reaction buffer (50 mM TrisHCl, pH 7.5, 150 mM NaCl), in the absence or in the presence of 5 mM $CaCl_2$ or EGTA. Each experiment started with a small injection of 1–2 µL, which was discarded from the analysis of the integrated data. Care was taken to start the first addition after baseline stability had been achieved. In each individual titration, 5 µL of a 850 µM MUPP1 peptide solution was injected into a solution of 50 µM CaM, using a computer-controlled 310- µL microsyringe. To allow the system to reach equilibrium, an interval of 240 s was applied between each ligand injection. Integrated heat data obtained for each titration were fitted using a nonlinear least-squares minimization algorithm to a theoretical titration curve, using the Origin package from the manufacturer. A model involving two sets of independent sites was used. ΔH (reaction enthalpy change, cal mol−1), K_A (binding constant, M−1) and N (stoichiometry) were the thermodynamic fitting parameters. K_D (dissociation constant) was calculated as the inverse of the association constant. The reaction entropy was calculated using the relationships $\Delta G = -RT\ln Ka$ (T = 298 K) and $\Delta G = \Delta H - T\Delta S$.

Funding

This work was funded by grants from: Università degli Studi di Padova (P-DiSC #01BIRD2018 to BM) (BIRD213814/21 to GMM); Fondazione Cassa di Risparmio di Padova e Rovigo (Progetti di Eccellenza 2011-2012), National Research Council of Italy and Ministero dell'Istruzione, dell'Universitá e della Ricerca (MIUR; EPIGEN Flagship project—Subproject 4), INsecTIME FP7 People: Marie-Curie Actions Initial Training Network (grant PITN-GA-2012-316790) to CR.

Figures

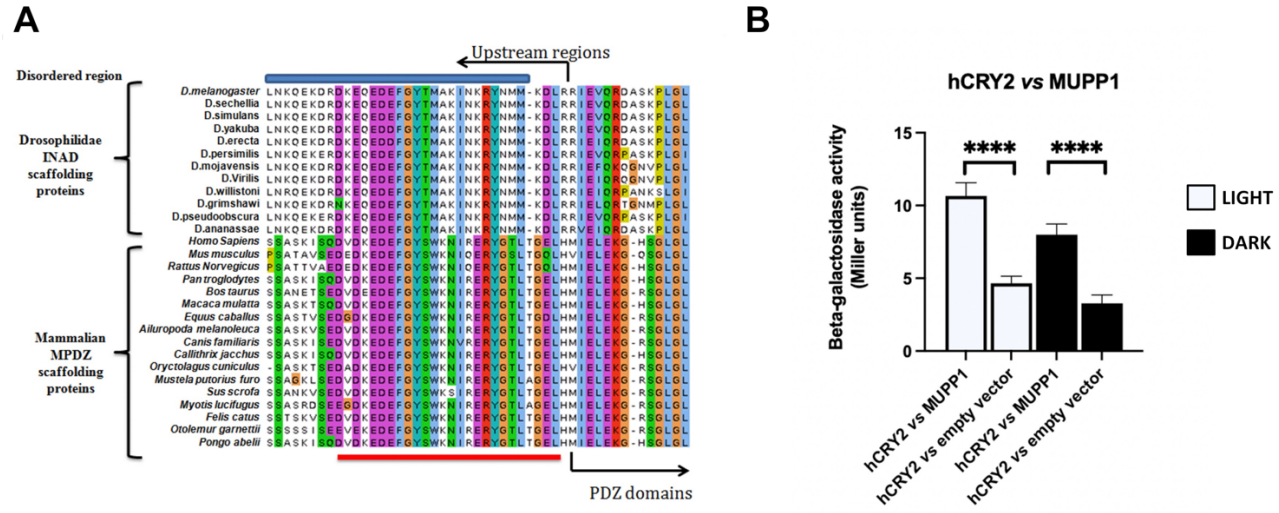

Figure 1 – A) Multiple sequence alignment of drosophilidae INAD-PDZ2 and mammalian MPDZ-PDZ8 upstream regions, colored using clustal color scheme. The blue bar on top highlights the predicted disordered region, while the red line on bottom marks the conserved pattern. B) hCRY2 interacts with MUPP1 both in light and dark. Yeast two-hybrid assay in which full-length hCRY2 (bait) was challenged with $hMUPP1_{1307-1564}$ (prey). As negative control, full-length hCRY2 was challenged with the empty prey vector. The mean ± SEM of seven independent clones, three replicates, are reported. **** p< 0,0001.

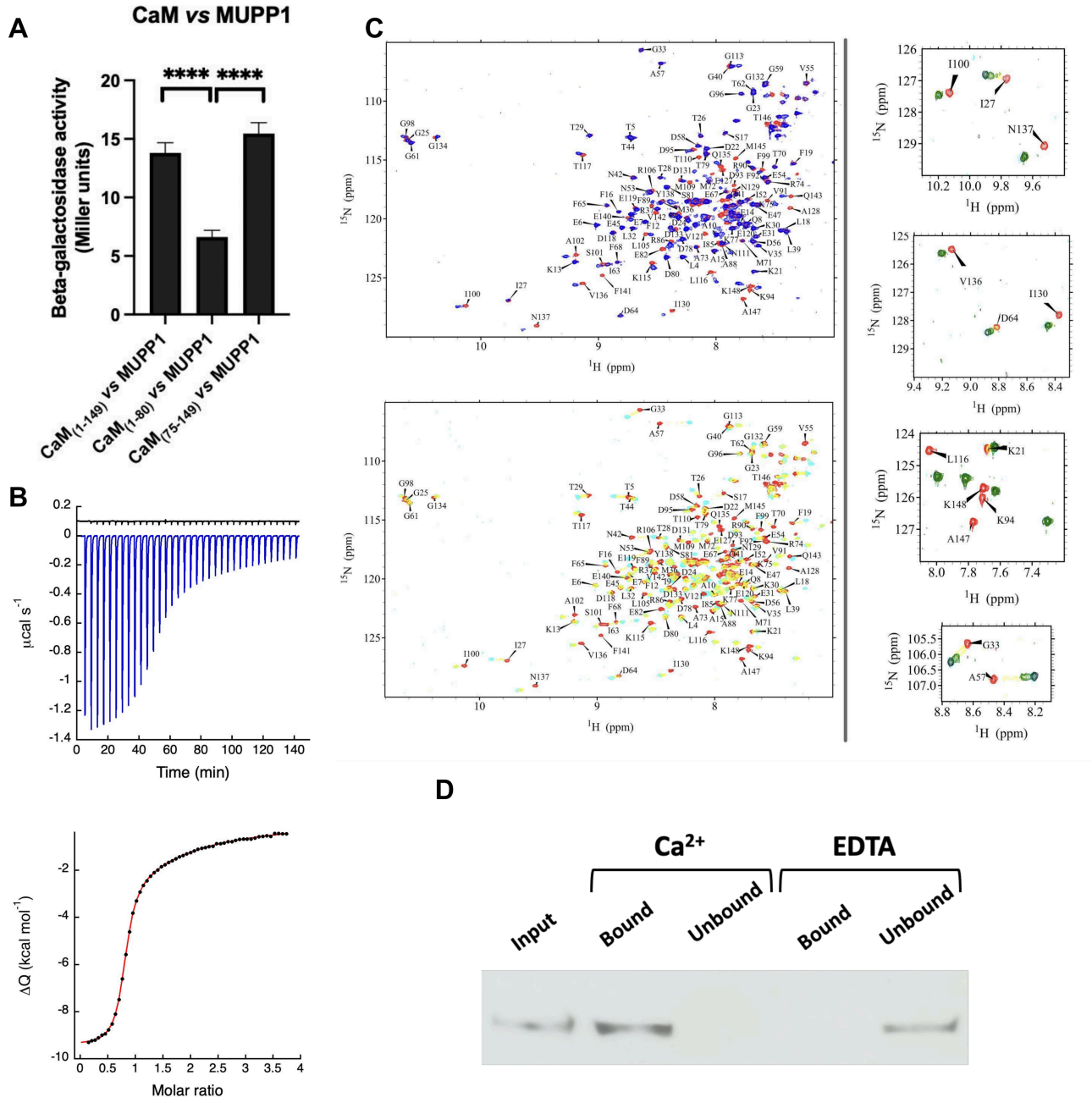

Figure 2

A) Yeast two-hybrid assay in which CaM (full-length or fragments) was challenged with hMUPP1(1307-1564). As negative control, CaM (full-length or fragments) was challenged with the empty prey vector, and the measured activity, considered as background, was subtracted from that of the samples. The mean ± SEM of seven independent clones, three replicates, are reported.

B) ITC measurements of the interaction between CaM and MUPP1 peptide. Raw titration data are represented in the top panel, representing the thermal effect of 57 × 5 µL injections of a solution of Mupp1 onto a solution of CaM, in the presence of 5 mM EGTA (upper black trace) or 5 mM Ca(II) (bottom blue trace). Normalized heats of reaction derived from the integration of raw data are reported in the bottom panel. The solid line represents the best fit of the data obtained using a nonlinear least-square fitting procedure using a binding model based on two sets of binding sites.

C) Superpositions of ^{15}N-HSQC spectra of ^{15}N-labeled calmodulin in the presence of increasing amounts of unlabeled MUPP1$_{1331-1343}$ peptide. Different peptide:CaM ratios are color coded as follows: 0:1 in red, 0.6:1 in blue, 1:1 in yellow, 1.3:1 in green, 2:1 in cyan, 2.5:1 in black). Top-left panel: ^{15}N-CaM spectra in the absence and in the presence of 0.6 equivalents of MUPP1$_{1331-1343}$ showing that only the C-terminal domain is

affected in the first part of the titration. Blue peaks represent the spectrum in presence of 0.6 equivalents of MUPP1$_{1331-1343}$, while red ones correspond to free CaM. Bottom-left panel: ^{15}N-CaM spectra in the absence and in presence of 1 and 2 equivalents of MUPP1$_{1331-1343}$. Right panels: enlargement of different regions of the spectra comparing the signals of free CaM with those upon the addition of 1.0, 1.3, 2.0 and 2.5 equivalents of peptide, showing that signals from the C-terminal domain are not significantly affected by the addition of more than 1 equivalent of MUPP1$_{1331-1343.}$-D) CaM pulldown assay and western blot showing the interaction between hMUPP1 and CaM. Protein extract from HEK-293T cells overexpressing MYC-hMUPP1 (input) was divided equally in two parts and the appropriate reagents were added ($CaCl_2$ or EDTA). Each extract (containing either $CaCl_2$ or EDTA) was incubated with CaM agarose beads to allow binding: unbound proteins were removed and the bound proteins were detached from the beads. Membranes were probed with an anti-MYC antibody. Different intensity of the bands is due to the different concentration of the proteins in the different samples.

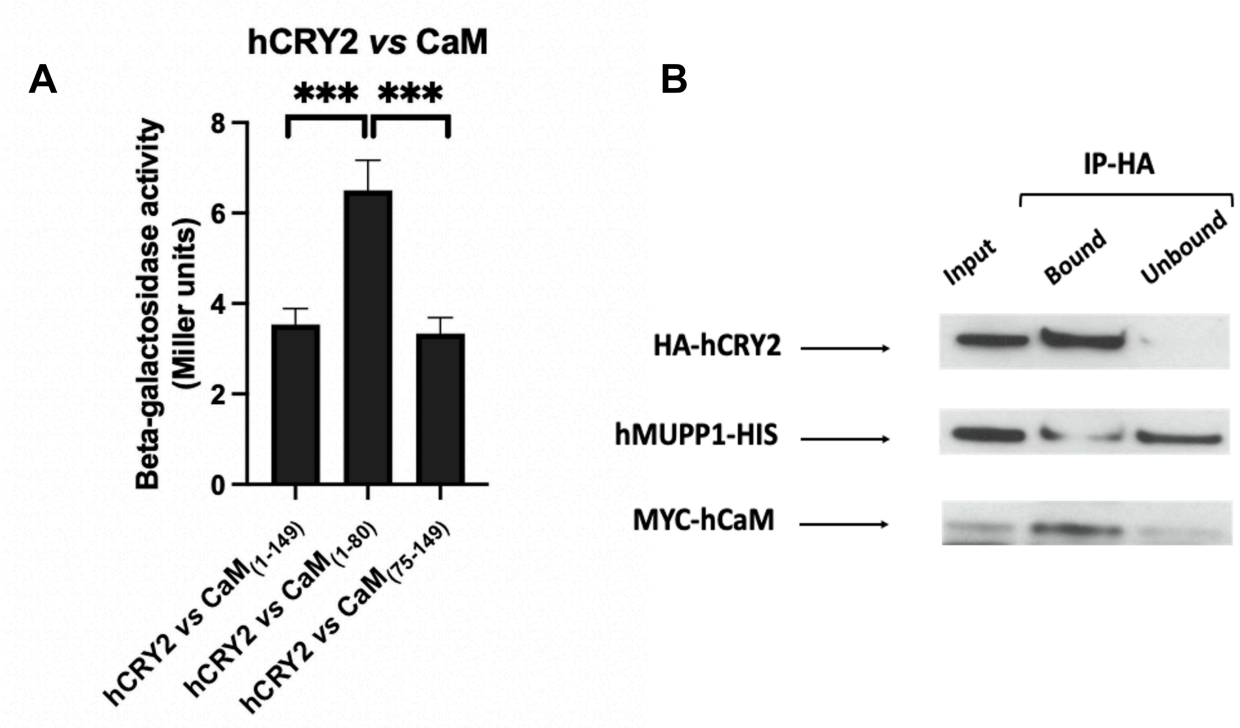

Figure 3. CaM forms a ternary complex with hCRY2 and MUPP1.
A) Yeast two-hybrid assay in which full-length hCRY2 was challenged with CaM (full-length or fragments). As negative control, full-length hCRY2 was challenged with the empty prey vector, and the measured activity, considered background, was subtracted from that of the samples. B) CoIP and western blot confirming the interaction between hCRY2, hMUPP1 and hCaM. Protein extract from Drosophila S2R+ cells overexpressing HA-CRY2, hMUPP1$_{1307-1564}$-HIS and MYC-hCAM (input) were incubated with HA-agarose beads to allow binding: unbound proteins were removed, and the bound proteins were detached from the beads. Membranes were probed with anti-HIS, anti-MYC anti-HA antibodies. Different intensity of the bands is due to the different concentration of the proteins in the different samples. Bands in the "UNBOUND" samples indicate that not the total amount of the proteins was involved in the binding.

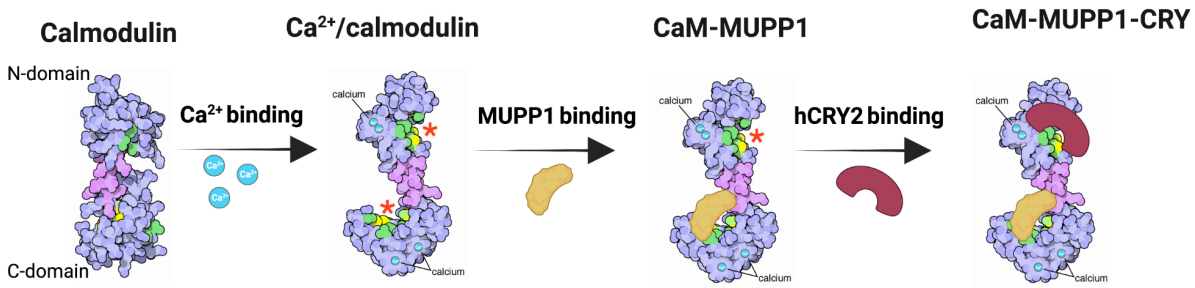

Figure 4. CaM serves as a bridge between hCRY2 and MUPP1.
In the presence of Ca2+, MUPP1 interacts with CaM's C-terminal lobe with high affinity. This observation suggests that the N-terminal lobe remains available for the interaction with hCRY2, thus forming a ternary complex. Created with BioRender.com (https://www.biorender.com).

References:

1. Deppisch P, Helfrich-Förster C, Senthilan PR (2022) The Gain and Loss of Cryptochrome/Photolyase Family Members during Evolution. Genes (Basel) 13:1613.
2. Michael AK, Fribourgh JL, Van Gelder RN, Partch CL (2017) Animal Cryptochromes: Divergent Roles in Light Perception, Circadian Timekeeping and Beyond. Photochem Photobiol 93:128–140.
3. Rosato E, Codd V, Mazzotta G, Piccin A, Zordan M, Costa R, Kyriacou CP (2001) Light-dependent interaction between Drosophila CRY and the clock protein PER mediated by the carboxy terminus of CRY. Curr. Biol. 11:909–917.
4. Busza A, Emery-Le M, Rosbash M, Emery P (2004) Roles of the two Drosophila CRYPTOCHROME structural domains in circadian photoreception. Science 304:1503–1506.
5. Dissel S, Codd V, Fedic R, Garner KJ, Costa R, Kyriacou CP, Rosato E (2004) A constitutively active cryptochrome in Drosophila melanogaster. Nat Neurosci 7:834–840.
6. Hemsley MJ, Mazzotta GM, Mason M, Dissel S, Toppo S, Pagano MA, Sandrelli F, Meggio F, Rosato E, Costa R, et al. (2007) Linear motifs in the C-terminus of D. melanogaster cryptochrome. Biochem. Biophys. Res. Commun. 355:531–537.
7. Ozturk N, Selby CP, Annayev Y, Zhong D, Sancar A (2011) Reaction mechanism of Drosophila cryptochrome. Proc. Natl. Acad. Sci. U.S.A. 108:516–521.
8. Gao P, Yoo S-H, Lee K-J, Rosensweig C, Takahashi JS, Chen BP, Green CB (2013) Phosphorylation of the cryptochrome 1 C-terminal tail regulates circadian period length. J Biol Chem 288:35277–35286.
9. Harada Y, Sakai M, Kurabayashi N, Hirota T, Fukada Y (2005) Ser-557-phosphorylated mCRY2 is degraded upon synergistic phosphorylation by glycogen synthase kinase-3 beta. J Biol Chem 280:31714–31721.
10. Damulewicz M, Mazzotta GM (2020) One Actor, Multiple Roles: The Performances of Cryptochrome in Drosophila. Front Physiol 11:99.
11. Emery P, So WV, Kaneko M, Hall JC, Rosbash M (1998) CRY, a Drosophila clock and light-regulated cryptochrome, is a major contributor to circadian rhythm resetting and photosensitivity. Cell 95:669–679.
12. Stanewsky R, Kaneko M, Emery P, Beretta B, Wager-Smith K, Kay SA, Rosbash M, Hall JC (1998) The cryb mutation identifies cryptochrome as a circadian photoreceptor in Drosophila. Cell 95:681–692.
13. Emery P, Stanewsky R, Hall JC, Rosbash M (2000) A unique circadian-rhythm photoreceptor. Nature 404:456–457.

14. Yoshii T, Funada Y, Ibuki-Ishibashi T, Matsumoto A, Tanimura T, Tomioka K (2004) Drosophila cryb mutation reveals two circadian clocks that drive locomotor rhythm and have different responsiveness to light. J Insect Physiol 50:479–488.
15. Rieger D, Shafer OT, Tomioka K, Helfrich-Förster C (2006) Functional analysis of circadian pacemaker neurons in Drosophila melanogaster. J Neurosci 26:2531–2543.
16. Dolezelova E, Dolezel D, Hall JC (2007) Rhythm defects caused by newly engineered null mutations in Drosophila's cryptochrome gene. Genetics 177:329–345.
17. Fogle KJ, Parson KG, Dahm NA, Holmes TC (2011) CRYPTOCHROME is a blue-light sensor that regulates neuronal firing rate. Science 331:1409–1413.
18. Fogle KJ, Baik LS, Houl JH, Tran TT, Roberts L, Dahm NA, Cao Y, Zhou M, Holmes TC (2015) CRYPTOCHROME-mediated phototransduction by modulation of the potassium ion channel β-subunit redox sensor. Proc Natl Acad Sci U S A 112:2245–2250.
19. Gegear RJ, Casselman A, Waddell S, Reppert SM (2008) Cryptochrome mediates light-dependent magnetosensitivity in Drosophila. Nature 454:1014–1018.
20. Yoshii T, Ahmad M, Helfrich-Förster C (2009) Cryptochrome mediates light-dependent magnetosensitivity of Drosophila's circadian clock. PLoS Biol 7:e1000086.
21. Fedele G, Green EW, Rosato E, Kyriacou CP (2014) An electromagnetic field disrupts negative geotaxis in Drosophila via a CRY-dependent pathway. Nat Commun 5:4391.
22. Marley R, Giachello CNG, Scrutton NS, Baines RA, Jones AR (2014) Cryptochrome-dependent magnetic field effect on seizure response in Drosophila larvae. Sci Rep 4:5799.
23. Bradlaugh AA, Fedele G, Munro AL, Hansen CN, Hares JM, Patel S, Kyriacou CP, Jones AR, Rosato E, Baines RA (2023) Essential elements of radical pair magnetosensitivity in Drosophila. Nature 615:111–116.
24. Ivanchenko M, Stanewsky R, Giebultowicz JM (2001) Circadian photoreception in Drosophila: functions of cryptochrome in peripheral and central clocks. J. Biol. Rhythms 16:205–215.
25. Krishnan B, Levine JD, Lynch MK, Dowse HB, Funes P, Hall JC, Hardin PE, Dryer SE (2001) A new role for cryptochrome in a Drosophila circadian oscillator. Nature 411:313–317.
26. Collins B, Mazzoni EO, Stanewsky R, Blau J (2006) Drosophila CRYPTOCHROME is a circadian transcriptional repressor. Curr. Biol. 16:441–449.
27. Schlichting M, Rieger D, Cusumano P, Grebler R, Costa R, Mazzotta GM, Helfrich-Förster C (2018) Cryptochrome Interacts With Actin and Enhances Eye-Mediated Light Sensitivity of the Circadian Clock in Drosophila melanogaster. Front Mol Neurosci 11:238.
28. van der Horst GT, Muijtjens M, Kobayashi K, Takano R, Kanno S, Takao M, de Wit J, Verkerk A, Eker AP, van Leenen D, et al. (1999) Mammalian Cry1 and Cry2 are essential for maintenance of circadian rhythms. Nature 398:627–630.
29. Shearman LP, Sriram S, Weaver DR, Maywood ES, Chaves I, Zheng B, Kume K, Lee CC, van der Horst GT, Hastings MH, et al. (2000) Interacting molecular loops in the mammalian circadian clock. Science 288:1013–1019.
30. Hirayama J, Nakamura H, Ishikawa T, Kobayashi Y, Todo T (2003) Functional and structural analyses of cryptochrome. Vertebrate CRY regions responsible for interaction with the CLOCK:BMAL1 heterodimer and its nuclear localization. J Biol Chem 278:35620–35628.
31. Sato TK, Yamada RG, Ukai H, Baggs JE, Miraglia LJ, Kobayashi TJ, Welsh DK, Kay SA, Ueda HR, Hogenesch JB (2006) Feedback repression is required for mammalian circadian clock function. Nat Genet 38:312–319.
32. Kiyohara YB, Tagao S, Tamanini F, Morita A, Sugisawa Y, Yasuda M, Yamanaka I, Ueda HR, van der Horst GTJ, Kondo T, et al. (2006) The BMAL1 C terminus regulates the circadian transcription feedback loop. Proc Natl Acad Sci U S A 103:10074–10079.
33. McCarthy EV, Baggs JE, Geskes JM, Hogenesch JB, Green CB (2009) Generation of a novel allelic series of cryptochrome mutants via mutagenesis reveals residues involved in protein-protein interaction and CRY2-specific repression. Mol Cell Biol 29:5465–5476.
34. Kang T-H, Lindsey-Boltz LA, Reardon JT, Sancar A (2010) Circadian control of XPA and

excision repair of cisplatin-DNA damage by cryptochrome and HERC2 ubiquitin ligase. Proc Natl Acad Sci U S A 107:4890–4895.
35. Lamia KA, Papp SJ, Yu RT, Barish GD, Uhlenhaut NH, Jonker JW, Downes M, Evans RM (2011) Cryptochromes mediate rhythmic repression of the glucocorticoid receptor. Nature 480:552–556.
36. Narasimamurthy R, Hatori M, Nayak SK, Liu F, Panda S, Verma IM (2012) Circadian clock protein cryptochrome regulates the expression of proinflammatory cytokines. Proc Natl Acad Sci U S A 109:12662–12667.
37. Kang T-H, Leem S-H (2014) Modulation of ATR-mediated DNA damage checkpoint response by cryptochrome 1. Nucleic Acids Research 42:4427–4434.
38. Sj P, Al H, Sd J, A K, M N, Jj M, Jr Y, Ka L (2015) DNA damage shifts circadian clock time via Hausp-dependent Cry1 stabilization. eLife [Internet] 4. Available from: https://pubmed.ncbi.nlm.nih.gov/25756610/
39. Mazzotta G, Rossi A, Leonardi E, Mason M, Bertolucci C, Caccin L, Spolaore B, Martin AJM, Schlichting M, Grebler R, et al. (2013) Fly cryptochrome and the visual system. PNAS 110:6163–6168.
40. Mazzotta GM, Bellanda M, Minervini G, Damulewicz M, Cusumano P, Aufiero S, Stefani M, Zambelli B, Mammi S, Costa R, et al. (2018) Calmodulin Enhances Cryptochrome Binding to INAD in Drosophila Photoreceptors. Front Mol Neurosci 11:280.
41. Manjunath GP, Ramanujam PL, Galande S (2018) Structure function relations in PDZ-domain-containing proteins: Implications for protein networks in cellular signalling. J Biosci 43:155–171.
42. Sitek B, Poschmann G, Schmidtke K, Ullmer C, Maskri L, Andriske M, Stichel CC, Zhu X-R, Luebbert H (2003) Expression of MUPP1 protein in mouse brain. Brain Res 970:178–187.
43. Krapivinsky G, Medina I, Krapivinsky L, Gapon S, Clapham DE (2004) SynGAP-MUPP1-CaMKII synaptic complexes regulate p38 MAP kinase activity and NMDA receptor-dependent synaptic AMPA receptor potentiation. Neuron 43:563–574.
44. Becamel C, Figge A, Poliak S, Dumuis A, Peles E, Bockaert J, Lubbert H, Ullmer C (2001) Interaction of serotonin 5-hydroxytryptamine type 2C receptors with PDZ10 of the multi-PDZ domain protein MUPP1. J Biol Chem 276:12974–12982.
45. Won S, Levy JM, Nicoll RA, Roche KW (2017) MAGUKs: multifaceted synaptic organizers. Curr Opin Neurobiol 43:94–101.
46. Zhu J, Shang Y, Zhang M (2016) Mechanistic basis of MAGUK-organized complexes in synaptic development and signalling. Nat Rev Neurosci 17:209–223.
47. Zhang J, Petit CM, King DS, Lee AL (2011) Phosphorylation of a PDZ domain extension modulates binding affinity and interdomain interactions in postsynaptic density-95 (PSD-95) protein, a membrane-associated guanylate kinase (MAGUK). J. Biol. Chem. 286:41776–41785.
48. Ernkvist M, Luna Persson N, Audebert S, Lecine P, Sinha I, Liu M, Schlueter M, Horowitz A, Aase K, Weide T, et al. (2009) The Amot/Patj/Syx signaling complex spatially controls RhoA GTPase activity in migrating endothelial cells. Blood 113:244–253.
49. Philipp S, Flockerzi V (1997) Molecular characterization of a novel human PDZ domain protein with homology to INAD from Drosophila melanogaster. FEBS Lett 413:243–248.
50. Lundkvist GB, Kwak Y, Davis EK, Tei H, Block GD (2005) A calcium flux is required for circadian rhythm generation in mammalian pacemaker neurons. J Neurosci 25:7682–7686.
51. Nahm S-S, Farnell YZ, Griffith W, Earnest DJ (2005) Circadian regulation and function of voltage-dependent calcium channels in the suprachiasmatic nucleus. J Neurosci 25:9304–9308.
52. Kon N, Yoshikawa T, Honma S, Yamagata Y, Yoshitane H, Shimizu K, Sugiyama Y, Hara C, Kameshita I, Honma K, et al. (2014) CaMKII is essential for the cellular clock and coupling between morning and evening behavioral rhythms. Genes Dev 28:1101–1110.
53. Jakubcakova V, Oster H, Tamanini F, Cadenas C, Leitges M, van der Horst GTJ, Eichele G (2007) Light entrainment of the mammalian circadian clock by a PRKCA-dependent posttranslational mechanism. Neuron 54:831–843.

598 54. Waterhouse AM, Procter JB, Martin DMA, Clamp M, Barton GJ (2009) Jalview Version 2--a
599 multiple sequence alignment editor and analysis workbench. Bioinformatics 25:1189–1191.
600 55. Notredame C, Higgins DG, Heringa J (2000) T-coffee: A novel method for fast and accurate
601 multiple sequence alignment. Journal of Molecular Biology 302:205–217.
602 56. Walsh I, Martin AJM, Di Domenico T, Vullo A, Pollastri G, Tosatto SCE (2011) CSpritz:
603 Accurate prediction of protein disorder segments with annotation for homology, secondary structure
604 and linear motifs. Nucleic Acids Research 39:W190–W196.
605 57. Dinkel H, Michael S, Weatheritt RJ, Davey NE, Van Roey K, Altenberg B, Toedt G, Uyar B,
606 Seiler M, Budd A, et al. (2012) ELM--the database of eukaryotic linear motifs. Nucleic Acids Res
607 40:D242-251.
608 58. Crooks GE (2004) WebLogo: A Sequence Logo Generator. Genome Research 14:1188–1190.
609 59. UniProt Consortium (2019) UniProt: a worldwide hub of protein knowledge. Nucleic Acids Res.
610 47:D506–D515.
611 60. Yap KL, Kim J, Truong K, Sherman M, Yuan T, Ikura M (2000) Calmodulin target database. J.
612 Struct. Funct. Genomics 1:8–14.
613 61. Bartel PL, Fields S The Yeast Two-hybrid System. Oxford University Press; 1997.
614 62. Ozgur S, Sancar A (2003) Purification and properties of human blue-light photoreceptor
615 cryptochrome 2. Biochemistry 42:2926–2932.
616 63. Ausbel F Current protocols in molecular biology. New York, NY, USA: In: Green Publishing
617 Associated; 1998.
618 64. Lee W, Tonelli M, Markley JL (2015) NMRFAM-SPARKY: enhanced software for biomolecular
619 NMR spectroscopy. Bioinformatics 31:1325–1327.
620